JCI The Journal of Clinical Investigation

Amendment history:
- Corrigendum (February 2023)
- Corrigendum (June 2020)

RANKL inhibition improves muscle strength and insulin sensitivity and restores bone mass

Nicolas Bonnet, … , Eleni Douni, Serge Ferrari

J Clin Invest. 2019. https://doi.org/10.1172/JCI125915.

Research In-Press Preview **Bone biology** **Muscle biology**

Receptor activator of Nfkb ligand (RANKL) activates, while osteoprotegerin (OPG) inhibits, osteoclastogenesis. In turn a neutralizing Ab against RANKL, denosumab improves bone strength in osteoporosis. OPG also improves muscle strength in mouse models of Duchenne's muscular dystrophy (*mdx*) and denervation-induce atrophy, but its role and mechanisms of action on muscle weakness in other conditions remains to be investigated. We investigated the effects of RANKL inhibitors on muscle in osteoporotic women and mice that either overexpress RANKL (*HuRANKL-Tg*$^{+}$), or lack *Pparb* and concomitantly develop sarcopenia (*Pparb*$^{-/-}$). In women, denosumab over 3 years improved appendicular lean mass and handgrip strength compared to no treatment, whereas bisphosphonate did not. *HuRANKL-Tg*$^{+}$ mice displayed lower limb force and maximal speed, while their leg muscle mass was diminished, with a lower number of type I and II fibers. Both OPG and denosumab increased limb force proportionally to the increase in muscle mass. They markedly improved muscle insulin sensitivity and glucose uptake, and decrease anti-myogenic and inflammatory […]

Original article:

RANKL inhibition improves muscle strength and insulin sensitivity and restores bone mass

One sentence summary:

RANK Ligand inhibitors improve muscle strength in post-menopausal women and muscle function and glucose metabolism in osteoporotic as well as sarcopenic mice.

Nicolas Bonnet[1], *Lucie Bourgoin*[1], *Emmanuel Biver*[1], *Eleni Douni*[2], *Serge Ferrari*[1]

1.Division of Bone Diseases, Department of Internal Medicine Specialties, Geneva University Hospital & Faculty of Medicine, Geneva 1205, Switzerland.

2.Biomedical Sciences Research Center "Alexander Fleming" Athens, Greece; Department of Biotechnology, Agricultural University of Athens, Athens, Greece

Corresponding Author: Nicolas Bonnet, 64 Av de la Roseraie, 1205 Geneva 14, nicolas.bonnet@unige.ch, Tel: + 41223729968; fax: + 41223829973

Conflict of interest:

No conflict of interest to disclose for NB, LB and EB

I received speaker and consulting honoraria from AMGEN for SF.

Abstract

Receptor activator of Nfkb ligand (RANKL) activates, while osteoprotegerin (OPG) inhibits, osteoclastogenesis. In turn a neutralizing Ab against RANKL, denosumab improves bone strength in osteoporosis. OPG also improves muscle strength in mouse models of Duchenne's muscular dystrophy (*mdx*) and denervation-induce atrophy, but its role and mechanisms of action on muscle weakness in other conditions remains to be investigated. We investigated the effects of RANKL inhibitors on muscle in osteoporotic women and mice that either overexpress RANKL (*HuRANKL-Tg+*), or lack *Pparb* and concomitantly develop sarcopenia *(Pparb*$^{-/-}$*)*. In women, denosumab over 3 years improved appendicular lean mass and handgrip strength compared to no treatment, whereas bisphosphonate did not. *HuRANKL-Tg+* mice displayed lower limb force and maximal speed, while their leg muscle mass was diminished, with a lower number of type I and II fibers. Both OPG and denosumab increased limb force proportionally to the increase in muscle mass. They markedly improved muscle insulin sensitivity and glucose uptake, and decrease anti-myogenic and inflammatory gene expression in muscle, such as myostatin and protein tyrosine phosphatase receptor-γ. Similarly, in *Pparb*$^{-/-}$, OPG increased muscle volume and force, while also normalizing their insulin signaling and higher expression of inflammatory genes in skeletal muscle. In conclusions, RANKL deteriorates, while its inhibitor improves, muscle strength and insulin sensitivity in osteoporotic mice and humans. Hence denosumab could represent a novel therapeutic approach for sarcopenia.

Introduction

Loss of bone and muscle mass and strength, i.e. osteoporosis and sarcopenia, often occurs concomitantly with aging, thereby increasing the risk of fragility fractures (*1-3*). Whereas several drugs are approved for treatment of osteoporosis, so far no therapy has been demonstrated to exert sufficiently positive effects on muscle to be approved for treatment of sarcopenia (*4*). Hence there is a need to better understand the molecular pathways involved in the loss of muscle mass and function and their potential relationship with osteoporosis, to eventually identify novel molecular targets for treatment of sarcopenia.

Increased expression of receptor activator of nuclear factor kappa-B ligand (RANKL) in post-menopausal women plays a central role in the development of osteoporosis (*5*). The binding of RANKL to its cognate receptor (RANK) leads to a cascade of signaling events triggering differentiation, activity and survival of osteoclasts (*6*). Osteoprotegerin (OPG) is a soluble decoy receptor which binding to RANKL prevents its interaction with RANK and thus restrains osteoclastogenesis and prevents bone loss (*7, 8*). In turn, a monoclonal antibody targeting RANKL, Denosumab (Dmab), has been shown to reduce fracture risk and is broadly used to treat osteoporosis (*9*). Interestingly, the rate of falls was also lower in subjects receiving Dmab compared to placebo, but this observation remains without a pathophysiological explanation (*10, 11*).

RANK is also expressed in skeletal muscle and activation of the Nfkb pathway mainly inhibits myogenic differentiation, which leads to skeletal muscle dysfunction and loss (*12, 13*). In turn OPG-Fc has been shown to reduce inflammation, restore the integrity and improve the function of dystrophic muscles in a mouse model of Duchenne's muscular dystrophy (*mdx* mice) (*14, 15*). In this model, RANK/RANKL/OPG controls calcium mobilization, apoptotic and inflammatory processes (*14, 15*).

Finally, another key function of the RANK/RANKL/OPG pathway is the regulation of glucose homeostasis. Blocking RANK activity in mouse liver protects against diet-induced glucose intolerance. On the contrary, direct stimulation of Nfkb pathway in primary hepatocytes exposed to RANKL triggers an upregulation of proinflammatory genes and Kupfer cells activation, both known to generate hepatic insulin resistance and affect overall glucose homeostasis. In this context, two recent papers suggest that circulating levels of OPG could be markers not only of bone metabolism, but also of impaired glucose regulation (*16, 17*).

These observations led us to hypothesize that RANKL inhibitors could exert a positive influence on muscle mass and strength, particularly in conditions of osteoporosis and/or sarcopenia, and their effects mediated by glucose regulation in these cells. For this purpose we first examined lean mass changes in a group of post-menopausal women with osteoporosis treated with denosumab or bisphosphonates. Having observed that only denosumab prevented the decline in lean mass and hand grip strength, we used transgenic mice expressing high copy numbers of human RANKL that develop severe osteoporosis (*18*), as well as *Pparb*$^{-/-}$ mice that develop a combination of osteo-/sarco-penia associated with an impairment of glucose homeostasis (*19*), to investigate the mechanisms by which RANKL inhibitors, denosumab and osteoprotegerin, could improve muscle function.

Results

Denosumab improves muscle mass and strength in postmenopausal women with osteoporosis

As a proof-of-concept, we first analysed the effects of denosumab (Dmab) in a group of post-menopausal women treated for osteoporosis for an average duration of 3 years, as compared to similar women without treatment or receiving bisphosphonate (BPs). BPs includes both alendronate and zoledronate treatments, for details see SI appendix. At baseline, lumbar spine areal bone mineral density (aBMD), BMI, and handgrip strength were similar between groups *(Supplemental table 1)*. Both Dmab and BPs improved aBMD compared to untreated (respectively +0.12±0.29g/cm^2 and +0.04±0.12g/cm^2 vs -0.07±0.19 g/cm^2, both $p<0.05$, Fig.1A). In contrast only Dmab increased appendicular lean mass (ALM) and handgrip strength (+0.66±2.2kg, +3.22±10.0kg, respectively, vs -0.06±0.39kg and -0.07±6.6kg, respectively, with BPS, and -0.36±1.03kg and -1.39±2.4kg, respectively, in untreated, both $p<0.05$, Fig.1B-C). Changes in ALM and handgrip strength were strongly correlated with changes in LS BMD ($r^2=0.82$ and $r^2=0.81$, both $p<0.001$, *Supplemental Fig.S1*) in the Dmab group but not in the other groups.

RANK-RANKL expression in skeletal muscle of wild type mice

To investigate whether RANKL inhibitors exert direct effects on muscle, we first assessed the level of RANK and RANKL mRNA expression in wild type (*WT*) mice. RANKL was indeed expressed at high levels in bone and muscle, particularly in the soleus, compared to other muscles (gastrocnemius) and other soft tissues including the intestine, liver, white and brown adipose tissues (WAT, BAT). RANK was also expressed in muscle, albeit at lower levels than in bone (Fig.2A, B). Immunohistochemistry and western-blot confirmed a higher protein expression of both RANK and RANKL in the soleus, i.e an oxidative muscle of predominantly type I fibers, than in gastrocnemius, i.e a mix of type I and II fibers (Fig.2C, D).

Effects of huRANKL overexpression on bone and muscle

We next investigated the effects of huRANKL overexpression on bone and muscle. In huRANKL transgenic mice, human RANKL expression levels were massively increased in bone and were approx. five times higher in the soleus compared to WT (Fig.2E). As previously reported, *huRANKLTg+* exhibit a severely decreased trabecular and cortical bone volume in both sexes (Fig.3A-B). Lower maximal speed and limb force in *huRANKLTg+* compared to *WT* remained only a trend after normalization by gastrocnemius mass arguing that decrease in functional parameters were mainly explained by muscle mass (Fig.3C-G). At 4 months of age, the *in vivo* muscle volume in the limb was lower whereas fat infiltration between muscle groups was higher in *huRANKLTg+* compared to *WT* (Fig.3F-J), which is a feature of sarcopenia. To investigate the mechanisms explaining the observed lower muscle mass/function, *huRANKLTg+* and *WT* littermates were hosted in metabolic cages during 24h. Despite similar food intake, *huRANKLTg+* showed lower fine movement compared to *WT* (Fig.3K). *huRANKLTg+* presented a lower CO_2 release, which remained significant when adjusted for lean mass *(Supplemental Fig.2A-E)*. Respiratory exchange ratio (RER) values close to 0.7 indicate that lipids are predominantly used as fuel sources upon carbohydrates in these mice *(Supplemental Fig.2A-E)*. Succinate dehydrogenase staining on skeletal muscle showed a decrease in both type I (dark blue) and II (light blue) fibers, confirmed by RTq-PCR showing a decrease in myosin I and II mRNA levels (Fig.3L-M). Moreover the soleus muscle of *huRANKLTg+* showed infiltration by mononucleated inflammatory cells and central nucleation of the myofibers, indicators of necrosis. Expression of genes related to fatty acid (FA) oxidation was lower (*Pparα, LPL*) whereas *myostatin* and *Ptp-Rg* mRNA levels were higher in *huRANKLTg+* compared to *WT* (Fig.3L-M, *Supplemental table 2*). In addition, multiplex analysis confirmed higher levels of TNF-α and IL1-β in *huRANKLTg+* compared to *WT*

specifically in the soleus (Fig. 3N). Other inflammatory cytokines such as IL-15, IL-6, mCSF, IFNγ, IL-10, Rantes, IL-1α, IL-17α were not significantly different between groups both in the soleus and gastrocnemius.

In addition to a certain degree of inflammation in muscles, the metabolic investigations indicated impaired glucose metabolism in these mice, as shown by a higher area under the curve of the ITT (Fig. 3O). Basic analyses of pancreas in *WT* and *HuRANKL-Tg+* mice, showed non-significant differences in the number and area of the islets as well as in insulin secretion *(Supplemental Fig.2F-H)*. At the muscular level, glucose uptake evaluated after 2-[^{14}C] deoxyglucose administration, was lower in the soleus of *huRANKLTg+* vs *WT* (Fig. 3P). In contrast, glucose uptake was increased in the femur of *huRANKL-Tg+* mice vs *WT*, probably due to the high bone remodeling levels induced by RANKL.

In summary, overexpression of RANKL decreased muscle mass, force, and glucose uptake associated with an upregulation of anti-myogenic and inflammatory genes.

RANKL induces insulin resistance in muscle cells through NF-kB signaling

To further evaluate the mechanism by which RANKL could affect glucose utilization in muscle specifically, we measured insulin receptor (IR) and AKT phosphorylation, which have been widely used as measures of insulin action, in C2C12 myotubes chronically exposed to RANKL or insulin (model of insulin resistance).

Acute insulin exposure increased phosphorylation of AKTser473, i.e a key node in insulin signalling propagation, and phospho-IRS1 on Ser318, known to prevent insulin receptor 1 activation. Chronic exposure to RANKL did not change the AKTser473 response to insulin but increased phosphorylation of IRS1 on Ser318. OPG-Fc had the opposite effects, namely decreased the activation of phospho-IRS1 on Ser318 in response to insulin (Fig.4A, *Supplemental Fig. 3A,B*). Since activation of Nfkb signalling is responsible for insulin

resistance in response to TNFα (*20*), we tested if it was also true in response to RANKL. In cell cultures exposed to acute insulin, OPG-Fc reversed the effects of chronic RANKL by blocking Nfkb signalling represented by the decreased mRNA expression of *Fos*, *Jun*, *NFAT* and *Ptp-RG*, without any effect on apoptotic markers (*Casp 3*, *Bcl2*) or calcium signalling (*Syk*) (Fig.4B). Most importantly, chronic RankL exposure increased glucose levels in the medium and OPG-Fc reversed this effect (Fig.4C), consistent with a re-activation of the insulin signalling pathway by OPG.

In the gold standard model of insulin resistance, i.e upon chronic insulin exposure, the expression of RANK-RANKL in C2C12 cells, as assessed by immunostaining, was increased *(Supplemental Fig. 3D*). In turn, AKT Ser473 phosphorylation in response to an acute bolus of insulin was blunted (Fig.4D). OPG-Fc treatment in the last 2 days was sufficient to partially restore AKT phosphorylation in these conditions (Fig.4D, *Supplemental Fig. 3E-F*). In addition, in these conditions and similarly to the observations above, OPG-Fc limits the phosphorylation of IR-Ser318, thereby improving insulin receptor activation. In accordance, after an acute exposure to insulin, chronic insulin exposure + OPG-Fc increased *Glut-1*, *Glut-4* and *Fabp4* gene expression *vs* chronic insulin exposure alone. In addition it decreased markers of inflammation and stress such *Tnfα*, *Ccl5* and *Fgf21*, as well as *Ptp-RG*, a key protein involved in Nfkb signaling, which was overexpressed under chronic insulin treatment (Fig.4E). Lastly, as expected under chronic insulin exposure, glucose levels in the medium were higher than in the controls. Addition of OPG-Fc significantly decreased glucose levels (Fig.4F).

It is important to note that the effects of OPG-Fc were only observed upon chronic exposure to RANKL or insulin, and not in their absence. This observation indicates that a certain level of RANKL and/ or insulin resistance is requested in order to see a significant impact of OPG-Fc on insulin sensitivity.

RANKL inhibitors restore muscle function and glucose utilization in huRANKL mice

Having established that RANKL impairs muscle functions and glucose uptake, and that OPG improves insulin signaling in C2C12 myotubes, we further examined the effects of RANKL inhibitors on muscle functions in mice in vivo. As expected OPG-Fc restored cortical bone volume by decreasing bone remodeling in *huRANKL* mice *(Supplemental Figure S4A-B).* OPG-Fc increase gastrocnemius mass, maximal force of the limb and maximal speed compared to *huRANKLTg+* vehicle (+9%, +21%, +44%, all $p<0.05$, Fig.5A). After adjustment by the gastrocnemius mass, maximal force of the limb and maximal speed differences between OPG-Fc and controls were no more significant (Fig.5B-C), arguing that the restauration of functional parameters was proportional to, and explained by, the improvement in muscle mass. Limb temperature of *huRANKLTg+* was improved by OPG-Fc suggesting a rescue of muscle energy expenditure (*Supplemental Figure S4C*). In accordance, both in soleus and gastrocnemius, the uptake of 2-[^{14}C] deoxyglucose was increased in response to OPG-Fc (Fig.5D) whereas no effect was seen in iWAT (Fig. 5D). Gene expression analysis showed an increased in markers of fatty acid (FA) oxidation and muscle fiber type I and II, as indicated by an upregulation of *Pparα*, *Myh1* & *2* and a decrease in *myostatin* and *Ptp-RG* in response to OPG-Fc, which is consistent to the changes observed in C2C12 *in vitro* (*Supplemental Figure S4D*). Accordingly, circulating levels of myostatin were reduced upon OPG-Fc treatment (*Supplemental Figure S4E*) and insulin resistance evaluated by an ITT was abolished (Fig.5E). Again, most of the effects of OPG-Fc seen in *huRANKLTg+* on bone structure and muscle function were not observed in *WT* mice, confirming that high levels of RANKL expression are both necessary and sufficient to induce muscle dysfunction.

Since OPG-Fc can have non-RANKL mediated activities, such as anti-apoptotic effects through Trails, we next treated the *huRANKLTg+* mice with the selective RANKL Ab, denosumab. As expected Dmab increased trabecular and cortical bone volume in these mice

and decreased bone remodeling (*Supplemental Figure S4F-H & Supplemental table 2&3*). Dmab increased gastrocnemius & soleus mass, maximal force of the limb and maximal speed compared to *huRANKLTg+* vehicle (+16%, +10%, +18% and +33%, all $p<0.05$, Fig.5F). Dmab effects on maximal speed remained significant after adjustment by gastrocnemius mass (Fig.5G-H), which would be consistent with an additional improvement in muscle metabolism, i.e. glucose uptake, independently of muscle mass. Spontaneous movement of the mice, more specifically fine movement, was also increased in Dmab treated mice (*Supplemental Figure S4I)*. Moreover, as with OPG-Fc, Dmab abolished the systemic insulin resistance observed in *huRANKLTg+* evaluated by ITT (Fig.5J). Gastrocnemius and soleus weights were higher under Dmab *vs* vehicle (respectively +9.3% and +12%, $p<0.05$, Fig.5H). 2-[^{14}C] deoxyglucose administration showed a higher glucose uptake in *huRANKLTg+* soleus and gastrocnemius treated by Dmab compared to vehicle (Fig.5I). Inversely, in the femur, the uptake was reduced by Dmab compared to vehicle, consistent with decreased bone remodeling. In accordance with the 2-[^{14}C] muscle uptake, the drop in the temperature of the limb observed in *huRANKLTg+* mice was rescued by Dmab (*Supplemental Figure S4J).* Western blot analysis indicated that the positive effects of Dmab on insulin signaling appear only in the soleus but not in the gastrocnemius *(Supplemental Figure S4K-L).* Lastly, in *huRANKLTg+* mice, succinate dehydrogenases staining indicated that Dmab switched type II fibers to type I and increased the fibers area of both type I and II fibers to levels similar to *WT* mice (*Supplemental Figure S5),* without significant changes in the number of fibers per section of muscle. Distribution of type I and II fibers were confirmed by immunohistochemistry *(Supplemental Figure S6).*

OPG-Fc restores muscle dysfunction and insulin resistance in osteo-sarcopenic Pparb$^{-/-}$ mice

To know whether the RANKL-RANK pathway could also be involved in sarcopenia, we took advantage of the *Pparb*$^{-/-}$ mice previously reported to develop bone fragility, muscle weakness and insulin resistance (*Supplemental table* 4).

At 5 months of age, *Pparb*$^{-/-}$ mice displayed reduced muscle volume and force normalized by gastrocnemius mass, respectively -19%, and -14% *vs WT* (Fig6.A-D, all $p<0.05$), associated with a lower limb temperature (-1.6% *vs WT* Fig.6E, $p<0.05$). Succinate dehydrogenase staining indicated lower number and area of type I fibers (Fig.6F1-3). ITT and GTT AUC were both higher in *Pparb*$^{-/-}$, +8% and +38% vs *WT* (Fig.6G-H both $p<0.05$). Western blot analysis confirmed an altered insulin response in muscles of *Pparb*$^{-/-}$ mice (Fig.6I). In the soleus, *Glut1*, *Fabp4*, *Ccm1*, *CyclinD1*, *Pgc1*α gene expression were downregulated (respectively -29%, -22%, -15%, -20% and -7%, *vs WT*, all $p<0.05$, Fig.6J), whereas markers of inflammation, *myostatin* / *Fgf21*, and *Nfkb* signalling, *Jun* / *NFAT* / *Ptp-RG* were upregulated (respectively +33%, +172%, +30%, +14% and +19% *vs* WT, all $p<0.05$, Fig.6J-K). OPG-Fc increased muscle volume (+12% vs Veh, $p<0.05$) and tended to increase the force, and temperature of the limb (respectively +6.7% and +1.8% vs Veh, Fig.6A-E). OPG-Fc also decreased GTT and ITT AUC (-36.7% and -22.3% *vs* Veh, $p<0.05$, Fig.6G-H) arguing for a restoration of systemic insulin sensitivity. Moreover, in soleus, gene expression of myosin I and II were increased whereas markers of inflammation myostatin and FGF21 were decreased by OPG-Fc in association with a decreased in gene related to Nfkb signalling (Fig.6J).

Discussion

Bone and muscle loss leading to osteoporosis and sarcopenia, respectively, are common features of aging (*2*). Together, they contribute to frailty and the risk of fragility fractures. Although the central role of the RANK/RANKL/OPG system on bone metabolism has been elucidated (*21*), leading to the development of a monoclonal Ab against RANKL (Dmab) to treat osteoporosis (*6*), the concomitant reduction in falls (*11*) and potential influence of these molecules on muscle metabolism in the context of osteoporosis and/or sarcopenia remain unexplained. Although there were no significant differences on bone or muscle parameters in osteoporotic post-menopausal women treated with Denosumab or bisphosphonates, only Denosumab significantly improved muscle strength compared to no treatment. In mice, high levels of huRANKL expression not only induced bone loss but concomitantly impaired muscle structure, strength and glucose uptake. These alterations are associated with increased expression of anti-myogenic / inflammatory markers in muscle, namely *myostatin* and *Ptp-RG*. The latter has previously been reported to cause insulin resistance in relation to inflammation in the liver (*22, 23*). However, compared to some models of muscle dystrophy (*24*), inflammation is not severe and inflammatory cytokines expression quite restricted in *huRANKL* mice, suggesting that it is not the main mechanism for muscle dysfunction in this model.

RANKL inhibitors such as OPG-Fc and Dmab corrected these abnormalities not only in *huRANKL* mice, but also in *Pparb*$^{-/-}$ osteo-sarcopenic mice, indicating that the RANKL-RANK system is ultimately involved in the development of muscle weakness irrespective of the triggering mechanism, i.e. whether directly mediated by increased RANKL or by deficiencies in more specific myogenic factors, such as Pparb. Taken together with recent evidence that conditional knockout for RANK in muscle prevented denervation-induced muscle weakness (*25*), our data now establish that the RANK/RANKL/OPG system plays a key role in muscle metabolism and the development of sarcopenia.

The effects of RANKL inhibition on muscle are likely direct, since we confirmed that RANK, as well as RANKL, are expressed in skeletal muscles and particularly in oxidative muscles like the soleus (*26*). In *WT* and transgenic mice we showed that the soleus is the 3rd tissue expressing the most RANKL and that high level of RANKL expression are sufficient to induce muscular alterations and a lower glucose uptake in skeletal muscle. When we compared the effects of OPG-Fc, *i.e* an inhibitor of both RANKL and TNF-related apoptosis-inducing ligand (TRAIL), with Denosumab, *i.e* a selective RANKL inhibitor, both treatments rescued muscle weakness to similar levels, suggesting an action on muscle mainly mediated through RANK signaling rather than TRAIL.

Our findings somewhat contrast with a recent publication which shows the superiority of OPG-Fc treatment to monoclonal anti-RANKL, anti-TRAIL or muscle RANK deletion in improving dystrophic muscle function *(27)*. However, our models of muscle weakness differ from the mdx mouse in that muscles were neither dystrophic nor markedly inflammatory in *huRANKL Tg+* nor *Pparb* KO mice. Consistent with our data, improving glucose entry into muscle through insulin sensitivity has been shown to improve muscle strength in two different mouse models of aging (*28*) and type 2 diabetes (Db/Db) (*29*).

To better understand the influence of RANKL-RANK signaling on muscle cells metabolism, we investigated insulin signaling in C2C12 differentiated myotubes expressing both RANK and RANKL (*15, 30*). In these cells RANKL increased, whereas OPG decreased, the level of IRS1 Ser318 phosphorylation, known to downregulate insulin receptor activity, while opposite effects were observed on AKTser 473 which is major activator of the IRS1. This was observed under both chronic RANKL and insulin exposure. Hence, these favorable effects of OPG on insulin receptor signaling were confirmed in vivo in both *huRANKLTg+* and *Pparb*$^{-/-}$ mice as suggested by the better ITT curves. In fat, TNFα-induced inflammation has previously shown

to attenuates IRS1 ability to transduce insulin signals, by the activation of IkB kinase β – Nfkb pathway (*20, 31*). More recently, protein tyrosine phosphatase receptor gamma (PTP-RG), has been highlighted as an important link between inflammation and insulin resistance in the liver. Here, we show that this link is also true in muscle where *Ptp-RG* is increased by RANKL, respectively decreased by OPG-Fc in C2C12 myotubes, and similarly decreased by Dmab in the soleus of *huRANKL Tg* mice (*23*). Hence, RANKL induces insulin signaling resistance, leading to poor glucose entry and in parallel induces a limited expression of inflammatory markers (such as *Ptp-RG* and *Tnfalpha*) that could then contribute further to decreased glucose uptake and muscle dysfunction (*20, 31*). Changes in glucose uptake in skeletal muscle have been previously described to lower contractile properties and muscle performance. In muscle-specific inducible Rac1 knockout mice for instance, 2-deoxyglucose uptake is blocked in soleus muscle and decreased by 80% and 60% in gastrocnemius and tibialis anterior muscles. One of the consequences is a significant reduction in maximal running speed (*32*).

In humans, beneficial effects of Denosumab on skeletal muscle function have previously been suggested in rare cases of muscular dystrophy (*33*). We have now extended this observation to more common osteoporotic subjects with muscle weakness, in which Dmab prevented the decrease in appendicular lean mass and grip strength over 3 years. Of note, the improvement of muscle function with Dmab was tightly correlated with BMD gains, whereas no correlation was present with BPs. These observations, although preliminary, seem to indicate that the improvement in muscle function with RANKL inhibitors occurs in parallel, but is not the consequence of the decrease in bone turnover achieved with bone anti-resorptives. This argues for a specific positive action of denosumab on muscles which could contribute to the 21% reduction of falls previously observed in the FREEDOM trials (*11*).

There are limitations to our study. First, we used a physiologically relevant and not muscle specific Tg mice overexpressing RANKL. Hence we cannot exclude that the improvement of systemic glucose metabolism, notably through the liver (*34*), and that neuronal or behavioral changes could also contribute to improve muscle function and particularly running speeds. However, the expression of RANK in C2C12 as well as the bulk of *in vitro* results indicating that OPG-Fc restores insulin receptor signaling, glucose uptake and gene expression in these cells, argues for a direct impact of RANKL inhibitors on muscle cells. Second, the test used for evaluation of maximal speed on the treadmill exhibit a higher variability than the other test because fatigue of the mice is based on a subjective operator appreciation and fatigue depend of several environmental factor. However, these results remain in accordance with the variability of similar tests in humans (CV=25%, (*35*)). Third, the number of human subjects treated by Denosumab was limited, and these subjects were not recruited on the base of sarcopenia. Hence a real prospective trial would be necessary to definitely establish the potential efficacy of Denosumab on muscle mass and function.

In summary, the RANK/RANKL/OPG system plays a key role not only in bone but also in muscle metabolism. Altogether our data point to a potentially new mechanism relating RANKL expression to fracture risk, i.e. not only by decreasing bone, but also muscle strength. Hence, this work opens a whole new opportunity to further investigate the potential benefits of RANKL inhibitors in the treatment of sarcopenia and frailty.

Materials and methods

In vivo experiment in mice. Osteoporotic *huRANKL Tg* mice (Tg5519 lines) expressing huRANKL were previously described (*18*). For adult phenotype description, OPG-Fc (truncated OPG-Fc with RankL domains only) and Denosumab treatment experiment see SI appendix. Micro-computed tomography scans, hyperinsulinemic-euglycemic clamp, 2-[^{14}C] deoxyglucose uptake, metabolic cage, positron emission tomography-computed tomography, histomorphometry, immunohistochemistry, multiplex ELISA, real-time PCR, western blotting, mechanical resistance of mouse femur were performed as described (*36-38*).

Cell culture. C2C12 myoblasts were cultured in growth medium (DMEM, 4.5 g/L glucose, 1% penicillin-streptomycin) supplemented with 10% FBS. Differentiation into myotubes was initiated by replacing growth medium by a differentiation medium (DMEM, 4.5 g/L glucose, 1% penicillin-streptomycin supplemented with 2% Horse serum) when cells reached 80% confluence. For western blot details see SI appendix.

Clinical investigation. 18 post-menopausal women (mean age 65.0±1.5 years) treated for osteoporosis with Dmab and 20 women treated by bisphosphonates (Alendronate n=8, Zoledronate n=12, mean age 65.7±0.9 years) were evaluated by DXA for body composition and for strength by handgrip and the time-to perform 5 chair lift before treatment and after 2.9[2.2-3.7] years of follow up as described (*39-41*). They were matched for analyses to 55 controls for age (mean age 65.0±1.4 years), BMI, BMD and fracture from the Geneva retired workers cohort (GERICO) (*41*).

Statistics. We tested the effects of genotype and treatment by a one or two way ANOVA. As appropriate, post hoc testing was performed using Fisher's protected Least Squares Difference

(PLSD). The effects of treatment in postmenopausal women was analysed by a Kruskal Wallis test. Differences were considered significant at $p < 0.05$. Data are presented as mean ± SEM.

Study approval.

All animal procedures were approved and carried out in strict accordance with the guidelines of the Institutional Animal Care and Use Committee and the canton of Geneva. Geneva Retirees Cohort protocol received the approval from the Geneva University Hospitals' Ethics Committee (GERICO, http://www.isrctn.com/ ISRCTN11865958), and all participants provided written informed consent.

Author contributions

Conceptualization: N.B, S.F; Methodology: N.B, L.B; Formal analysis and investigation: L.B, E.B, N.B; Writing - original draft preparation: N.B; Writing - review and editing: N.B, L.B, E.B, E.D, S.F; Funding acquisition: N.B, S.F; Resources: N.B, S.F, E.D; Supervision: N.B.

Acknowledgments

We thank Ms Madeleine Lachize, Julia Brun and Juliette Cicchini for her technical assistance; T. Chevalley, M. Hars, A. Trombetti for contributing to the collection of data in the GERICO cohort. These studies were supported by a Swiss National Science Foundation grant No 3100A0-116633/1 (to SF). This work was further supported by a grant from the EFSD (to N.B). The authors declare no competing financial interests.

References

1. Cartwright MJ, Tchkonia T, Kirkland JL, Aging in adipocytes: potential impact of inherent, depot-specific mechanisms. *Exp Gerontol.* **42**, 463-471 (2007).
2. Rosen CJ, Bouxsein ML, Mechanisms of disease: is osteoporosis the obesity of bone? *Nat Clin Pract Rheumatol.* **2**, 35-43 (2006).
3. Viña J, Rodriguez-Mañas L, Salvador-Pascual A, Tarazona-Santabalbina FJ, Gomez-Cabrera MC, Exercise: the lifelong supplement for healthy ageing and slowing down the onset of frailty. *J Physiol.* **594**, 1989-1999 (2016).
4. Maurel DB, Jähn K, Lara-Castillo N, Muscle-Bone Crosstalk: Emerging Opportunities for Novel Therapeutic Approaches to Treat Musculoskeletal Pathologies. *Biomedicines* **5**, doi: 10.3390 (2017).
5. Eghbali-Fatourechi G, Khosla S, Sanyal A, Boyle WJ, Lacey DL, Riggs BL, Role of RANK ligand in mediating increased bone resorption in early postmenopausal women. *J Clin Invest.* **111**, 1221-1230 (2003).
6. Lacey DL, Boyle WJ, Simonet WS, Kostenuik PJ, Dougall WC, Sullivan JK, San Martin J, Dansey R, Bench to bedside: elucidation of the OPG-RANK-RANKL pathway and the development of denosumab. *Nat Rev Drug Discov.* **11**, 401-419 (2012).
7. Ominsky MS, Li X, Asuncion FJ, Barrero M, Warmington KS, Dwyer D, Stolina M, Geng Z, Grisanti M, Tan HL, Corbin T, McCabe J, Simonet WS, Ke HZ, Kostenuik PJ, RANKL inhibition with osteoprotegerin increases bone strength by improving cortical and trabecular bone architecture in ovariectomized rats. *J Bone Miner Res.* **23**, 672-682 (2008).
8. Simonet WS, Lacey DL, Dunstan CR, Kelley M, Chang MS, Lüthy R, Nguyen HQ, Wooden S, Bennett L, Boone T, Shimamoto G, DeRose M, Elliott R, Colombero A, Tan HL, Trail G, Sullivan J, Davy E, Bucay N, Renshaw-Gegg L, Hughes TM, Hill D, Pattison W, Campbell P, Sander S, T. Van G, arpley J, Derby P, Lee R, Boyle WJ, Osteoprotegerin: a novel secreted protein involved in the regulation of bone density. *Cell* **89**, 309-319 (1997).
9. McCloskey EV, Johansson H, Oden A, Austin M, Siris E, Wang A, Lewiecki EM, Lorenc R, Libanati C, Kanis JA, Denosumab reduces the risk of osteoporotic fractures in postmenopausal women, particularly in those with moderate to high fracture risk as assessed with FRAX. *J Bone Miner Res.* **27**, 1480-1486 (2012).
10. Huang J, Hsu YH, Mo C, Abreu E, Kiel DP, Bonewald LF, Brotto M, Karasik D, METTL21C is a potential pleiotropic gene for osteoporosis and sarcopenia acting through the modulation of the NF-κB signaling pathway. *J Bone Miner Res.* **29**, 1531-1540 (2014).
11. Lewiecki EM, Safety and tolerability of denosumab for the treatment of postmenopausal osteoporosis. *Drug Healthc Patient Saf.* **3**, 79-91 (2011).
12. Langen RC, Schols AM, Kelders MC, Wouters EF, Janssen-Heininger YM, Inflammatory cytokines inhibit myogenic differentiation through activation of nuclear factor-kappaB. *FASEB J.* **15**, 1169-1180 (2001).
13. Lee D, Goldberg AL, Muscle Wasting in Fasting Requires Activation of NF-κB and Inhibition of AKT/Mechanistic Target of Rapamycin (mTOR) by the Protein Acetylase, GCN5. *J Biol Chem.* **290**, 30269-30279 (2015).
14. Dufresne SS, Dumont NA, Bouchard P, Lavergne É, Penninger JM, Frenette J, Osteoprotegerin protects against muscular dystrophy. *Am J Pathol.* **185**, 920-926 (2015).
15. Dufresne SS, Dumont NA, Boulanger-Piette A, Fajardo VA, Gamu D, Kake-Guena SA, David RO, Bouchard P, Lavergne É, Penninger JM, Pape PC, Tupling AR, Frenette J, A. 15, ():. Muscle RANK is a key regulator of Ca2+ storage, SERCA activity, and function of fast-twitch skeletal muscles. *Am J Physiol Cell Physiol.* **310**, C663-672 (2016).
16. Mashavi M, Menaged M, Shargorodsky M, Circulating osteoprotegerin in postmenopausal osteoporotic women: marker of impaired glucose regulation or impaired bone metabolism. *Menopause* **24**, 1264-1268 (2017).
17. Duan P, Yang M, Wei M, Liu J, Tu P, Serum Osteoprotegerin Is a Potential Biomarker of Insulin Resistance in Chinese Postmenopausal Women with Prediabetes and Type 2 Diabetes. *Int J Endocrinol.* **10.1155** 8724869 (2017).
18. Rinotas V, Niti A, Dacquin R, Bonnet N, Stolina M, Han CY, Kostenuik P, Jurdic P, Ferrari S, Douni E, Novel genetic models of osteoporosis by overexpression of human RANKL in transgenic mice. *J Bone Miner Res.* **29**, 1158-1169 (2014).
19. Fu H, Desvergne B, Ferrari S, Bonnet N, Impaired Musculoskeletal Response to Age and Exercise in PPARβ-/- Diabetic Mice. *Endocrinology* **155**, 4686-4696 (2014).

20. Hotamisligil GS, Peraldi P, Budavari A, Ellis R, White MF, Spiegelman BM, IRS-1-mediated inhibition of insulin receptor tyrosine kinase activity in TNF-alpha- and obesity-induced insulin resistance. *Science* **271**, 665-668 (1996).
21. Kearns AE, Khosla S, Kostenuik PJ, Receptor activator of nuclear factor kappaB ligand and osteoprotegerin regulation of bone remodeling in health and disease. *Endocr Rev.* **29**, 155-192 (2008).
22. Guo T, Bond ND, Jou W, Gavrilova O, Portas J, McPherron AC, Myostatin inhibition prevents diabetes and hyperphagia in a mouse model of lipodystrophy. *Diabetes* **61**, 2414-2423 (2012).
23. Brenachot X, Ramadori G, Ioris RM, Veyrat-Durebex C, Altirriba J, Aras E, Ljubicic S, Kohno D, Fabbiano S, Clement S, Goossens N, Trajkovski M, Harroch S, Negro F, Coppari R, Hepatic protein tyrosine phosphatase receptor gamma links obesity-induced inflammation to insulin resistance. *Nat Commun.* **8**, s41467-41017-02074-41462 (2017).
24. Dong H, Huang H, Yun X, Kim DS, Yue Y, Wu H, Sutter A, Chavin KD, Otterbein LE, Adams DB, Kim YB, Wang H, Bilirubin increases insulin sensitivity in leptin-receptor deficient and diet-induced obese mice through suppression of ER stress and chronic inflammation. *Endocrinology* **155**, 818-828 (2014).
25. Dufresne SS, Boulanger-Piette A, Bossé S, Frenette J, Physiological role of receptor activator nuclear factor-kB (RANK) in denervation-induced muscle atrophy and dysfunction. *Receptors Clin Investig.* **3**, e13231-e13236 (2016).
26. Marciano DP, Kuruvilla DS, Boregowda SV, Asteian A, Hughes TS, Garcia-Ordonez R, Corzo CA, Khan TM, Novick SJ, Park H, Kojetin DJ, Phinney DG, Bruning JB, Kamenecka TM, Griffin PR, Pharmacological repression of PPARγ promotes osteogenesis. *Nat Commun.* **6**, (2015).
27. Dufresne SS, Boulanger-Piette A, Bossé S, Argaw A, Hamoudi D, Marcadet L, Gamu D, Fajardo VA, Yagita H, Penninger JM, Russell Tupling A, Frenette J, Genetic deletion of muscle RANK or selective inhibition of RANKL is not as effective as full-length OPG-fc in mitigating muscular dystrophy. *Acta Neuropathol Commun.* **6**, 31 (2018).
28. Camporez JP, Petersen MC, Abudukadier A, Moreira GV, Jurczak MJ, Friedman G, Haqq CM, Petersen KF, Shulman GI, Anti-myostatin antibody increases muscle mass and strength and improves insulin sensitivity in old mice. *Proc Natl Acad Sci U S A.* **113**, 2212-2217 (2016).
29. Jiang JG, Shen GF, Li J, Qiao C, Xiao B, Yan H, Wang DW, Xiao X, Adeno-associated virus-mediated expression of myostatin propeptide improves the growth of skeletal muscle and attenuates hyperglycemia in db/db mice. *Gene Ther.* **24**, 167-175 (2017).
30. Park HJ, Baek K, Baek JH, Kim HR, TNFα Increases RANKL Expression via PGE_2-Induced Activation of NFATc1. *Int J Mol Sci.* **18**, doi: 10.3390 (2017).
31. Aguirre V, Werner ED, Giraud J, Lee YH, Shoelson SE, White MF, Phosphorylation of Ser307 in insulin receptor substrate-1 blocks interactions with the insulin receptor and inhibits insulin action. *J Biol Chem.* **277**, 1531-1537 (2002).
32. Sylow L, Nielsen IL, Kleinert M, Møller LL, Ploug T, Schjerling P, Bilan PJ, Klip A, Jensen TE, Richter EA, Rac1 governs exercise-stimulated glucose uptake in skeletal muscle through regulation of GLUT4 translocation in mice. *J Physiol.* **594**, 4997-5008 (2016).
33. Lefkowitz SS, Lefkowitz DL, Kethley J, Treatment of facioscapulohumeral muscular dystrophy with Denosumab. *Am J Case Rep.* **13**, 66-68 (2012).
34. Kiechl S, Wittmann J, Giaccari A, Knoflach M, Willeit P, Bozec A, Moschen AR, Muscogiuri G, Sorice GP, Kireva T, Summerer M, Wirtz S, Luther J, Mielenz D, Billmeier U, Egger G, Mayr A, Oberhollenzer F, Kronenberg F, Orthofer M, Penninger JM, Meigs JB, Bonora E, Tilg H, Willeit J, Schett G, Blockade of receptor activator of nuclear factor-κB (RANKL) signaling improves hepatic insulin resistance and prevents development of diabetes mellitus. *Nat Med.* **19**, 358-363 (2013).
35. Billat V, Renoux JC, Pinoteau J, Petit B, Koralsztein JP, Reproducibility of running time to exhaustion at VO2max in subelite runners. *Med Sci Sports Exerc.* **26**, 254-257 (1994).
36. Bonnet N, Conway SJ, Ferrari SL, Regulation of beta catenin signaling and parathyroid hormone anabolic effects in bone by the matricellular protein periostin. *Proc Natl Acad Sci U S A.* **109**, 15048-15053 (2012).
37. Bourgoin L, Peyrou M, Poher AL, Altirriba J, Maeder C, Caillon A, Fournier M, Montet X, Rohner-Jeanrenaud F, Foti M, Hepatic PTEN deficiency improves muscle insulin sensitivity and decreases adiposity in mice. *J Hepatol.* **62**, 421-429 (2015).
38. Suárez-Zamorano N, Fabbiano S, Chevalier C, Stojanović O, Colin DJ, Stevanović A, Veyrat-Durebex C, Tarallo V, Rigo D, Germain S, Ilievska M, Montet X, Seimbille Y, Hapfelmeier S, Trajkovski M, Microbiota depletion promotes browning of white adipose tissue and reduces obesity. *Nat Med.* **21**, 1497-1501 (2015).
39. Trombetti A, Reid KF, Hars M, Herrmann FR, Pasha E, Phillips EM, Fielding RA, Age-associated declines in muscle mass, strength, power, and physical performance: impact on fear of falling and quality of life. *Osteoporos Int.* **27**, 463-471 (2016).

40. Hars M, Biver E, Chevalley T, Herrmann F, Rizzoli R, Ferrari S, Trombetti A, Low Lean Mass Predicts Incident Fractures Independently From FRAX: a Prospective Cohort Study of Recent Retirees. *J Bone Miner Res.* **31**, 2048-2056 (2016).
41. Bonnet N, Biver E, Chevalley T, Rizzoli R, Garnero P, Ferrari SL, Serum Levels of a Cathepsin-K Generated Periostin Fragment Predict Incident Low-Trauma Fractures in Postmenopausal Women Independently of BMD and FRAX. *J Bone Miner Res.* **doi: 10.1002**, (2017).

Figures and figure legends

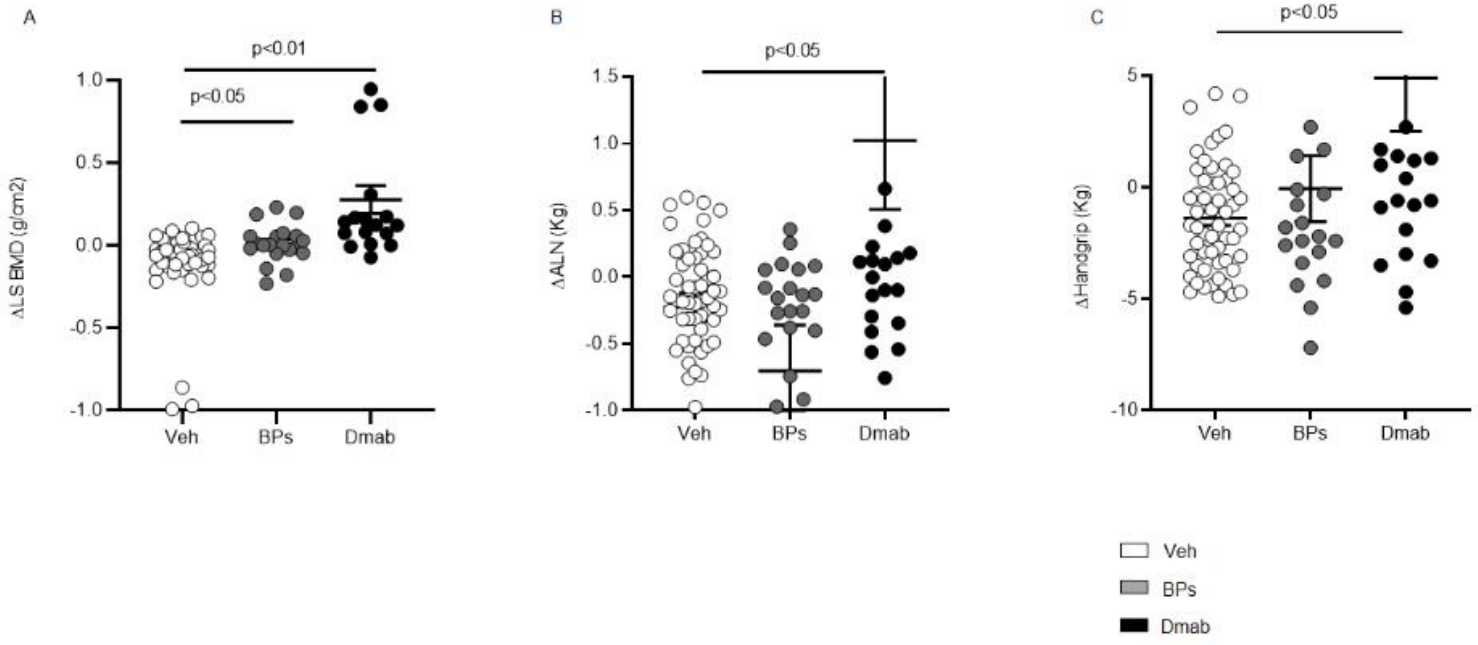

Fig. 1

Figure 1. Bone mineral density, appendicular lean mass and handgrip of post-menopausal osteoporotic women before and after 3 years of bisphosphonates or denosumab treatment. (A) delta lumber spine bone mineral density (ΔLS BMD). (B) Appendicular lean mass (ΔALN). (C) delta handgrip. Control (n=55), bisphosphonates (BPs, n=20), Denosumab (Dmab, n=18). Statistical differences were assessed by a Kruskal Wallis test. Bars show means (± SD).

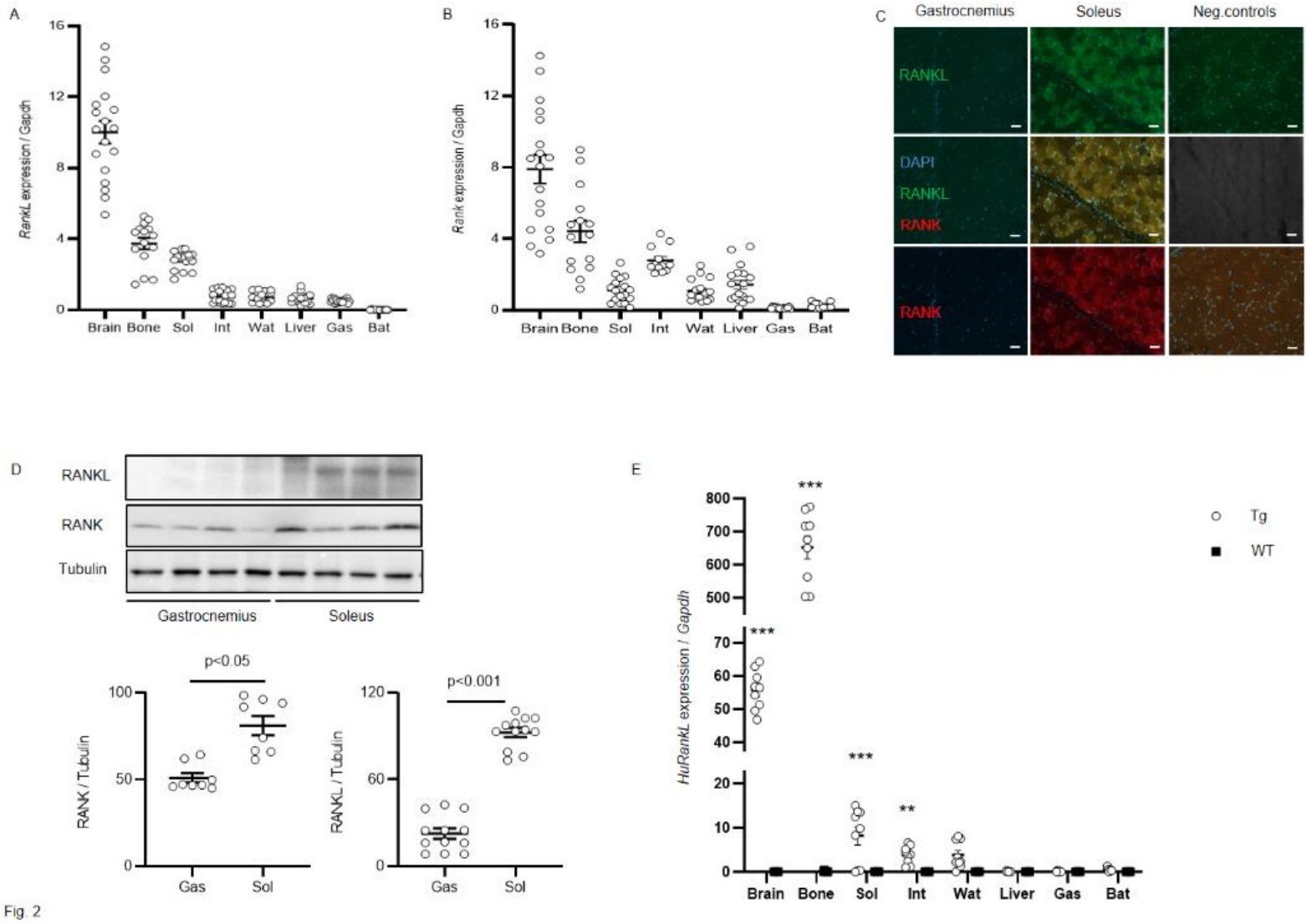

Figure 2. Distribution of RANK and RANKL in tissue. (A-B) Relative mRNA gene expression of RANKL and RANK in mice aged of 4 weeks (n=12-18). Soleus (Sol), Intestin (Int), White adipose tissue (WAT), Gastrocnemius (Gas), Brown adipose tissue (BAT). (C) Immunohistochemical staining of Dapi, RANK, RANKL in gastrocnemius and soleus, scale bars represent 50µm. (D) Western blot of RANK and RANKL in gastrocnemius and soleus. Bars show means (± SEM). (E) Relative mRNA gene expression of human RANKL in WT (square) and huRANKLTg+ (Tg, circle). ** P<0.01, *** P<0.001 significant difference vs. *WT*. Statistical differences were assessed by one way ANOVA.

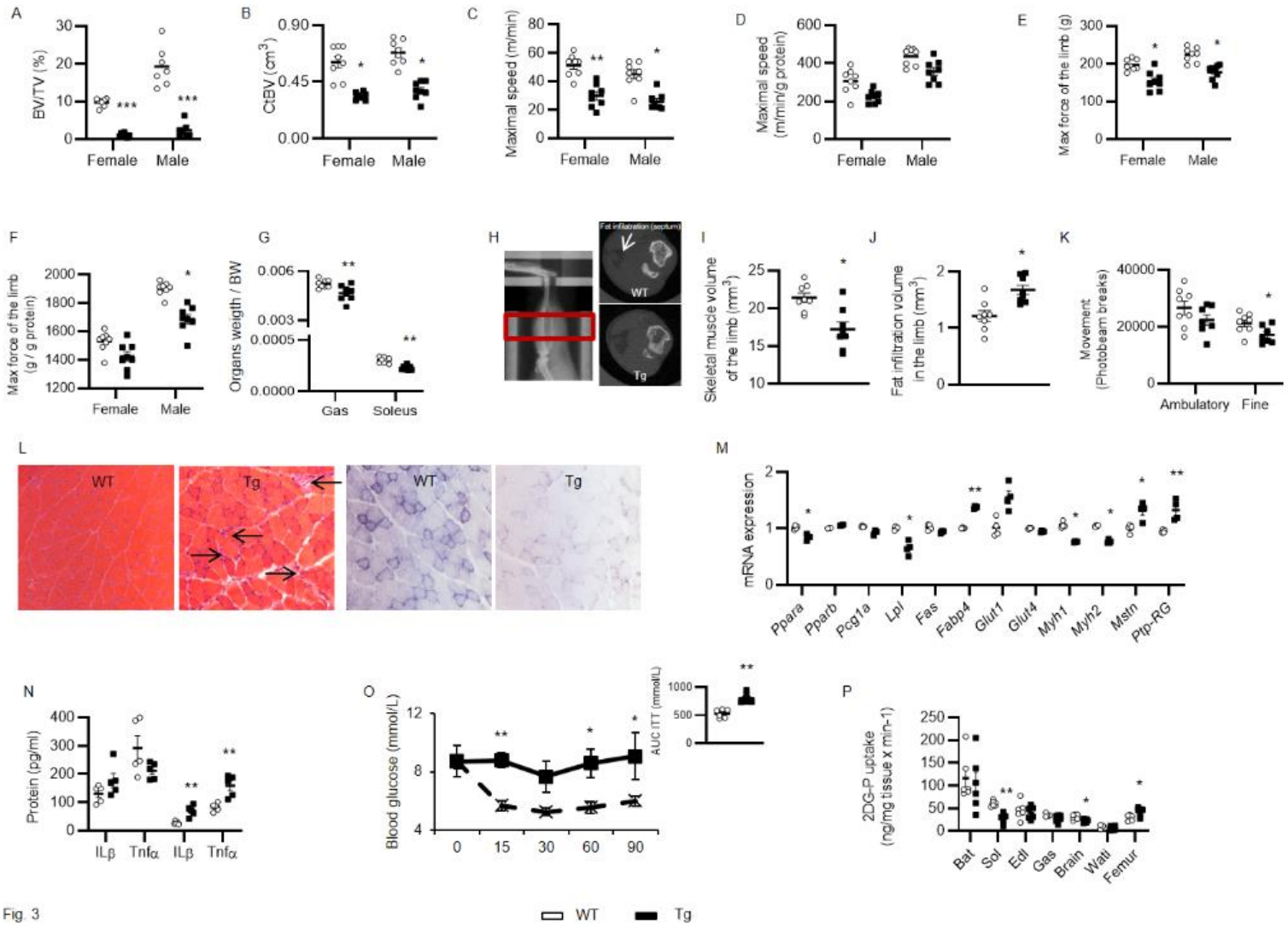

Fig. 3

Figure 3. Bone, muscle and glucose phenotype of huRANKLTg+ (Tg). (A-B) Trabecular bone volume on tissue volume (BV/TV) at the distal femur and cortical bone volume (Ct.BV) at midshaft femur (*n* = 8 per group). (C) Absolute value of maximal speed evaluated on treadmill. (D) Maximal speed normalized by gastrocnemius mass. (E) Limb force evaluated by handgrip (*n* = 8 per group). (F) Limb force normalized by gastrocnemius mass. (G) Female skeletal muscle weight normalized by body weight (BW). (H-J) Skeletal muscle volume of the limb and fat infiltration evaluated by in vivo microCT. (K) Movement record in metabolic cages during two consecutive days and nights (*n* = 6 per group). Ambulatory represent displacement activity, Fine represent activity without any ground displacement (L) Haematoxylin eosin (H&E) and Succinate dehydrogenase staining on sections of soleus, arrow indicate mononucleated inflammatory cells and central nucleation of the myofibers which are indicators of necrosis (*n* = 6 per group with 2 sections per animals; bar = 50 µm). (M) Relative mRNA gene expression in soleus (*n* = 4 per group). (N) Inflammatory cytokines in gastrocnemius and soleus muscle. (O) Insulin tolerance test (ITT), area under the curve (AUC) (*n* = 6 per group). (P) Tissue specific 2-[14C]deoxyglucose (2-[14C]DG) in brown adipose tissue (BAT), soleus (Sol), extensor digitorum longus (Edl), Gastrocnemius (Gas), inguinal WAT (Wati) of huRANKLTg+ (*n* = 6 per group). Statistical differences were assessed by one way ANOVA.* *P*<0.05, ** *P*<0.01, *** *P*<0.001 significant difference vs. WT. Bars show means (± SEM). Closed bars, huRANKLTg+ ; open bars, *WT*.

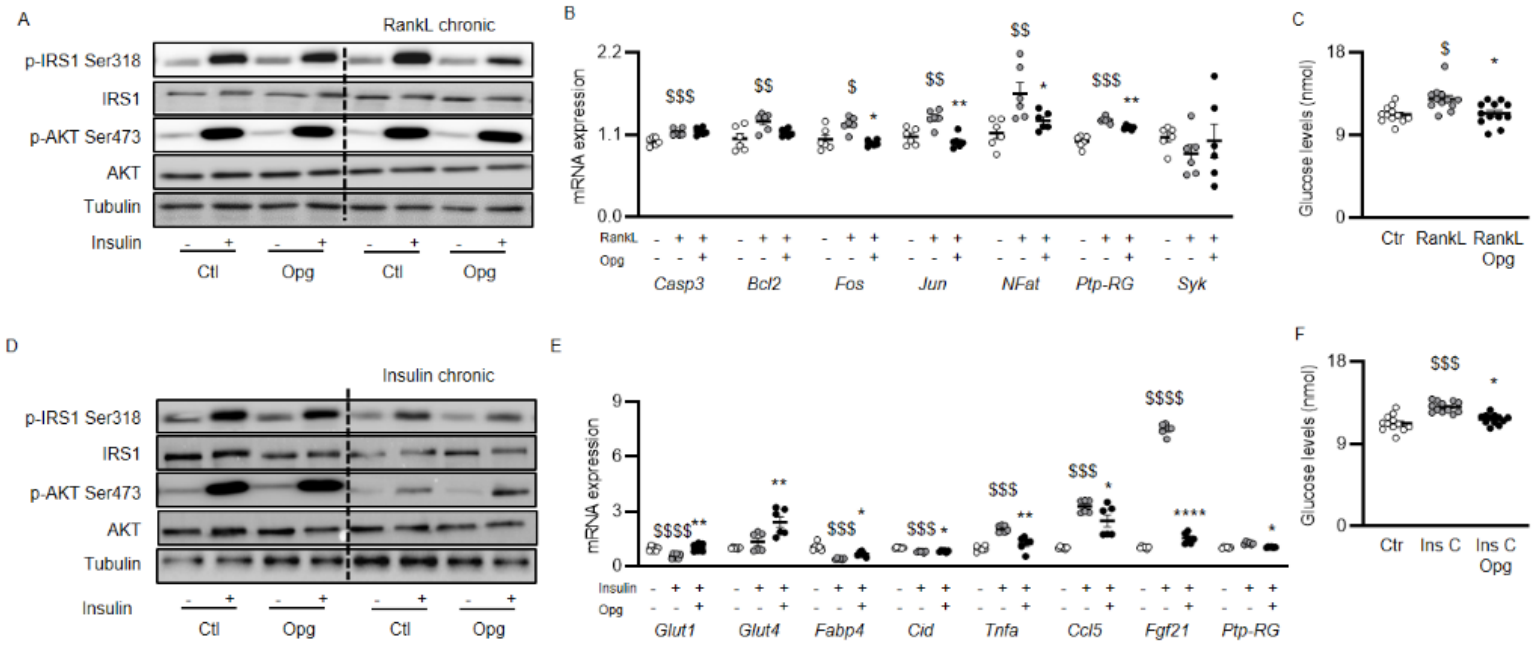

Fig. 4

Figure 4. In C2C12 cell line, OPG-Fc decreased insulin resistant, inflammation and glucose levels in the medium in a model of chronic RANKL and insulin. (A-C) C2C12 culture after differentiation into myotube and under a chronic exposure to RANKL ± OPG-Fc and in response to an acute exposure to insulin, (A) western blot (n=3), (B) relative mRNA gene expression (n=6), (C) glucose levels in medium (n=6). (D-F) C2C12 culture after differentiation into myotube and under a chronic exposure to insulin ± OPG-Fc and in response to an acute exposure to insulin, (D) western blot (n=3), (E) relative mRNA gene expression (n=6), (F) glucose levels in medium (n=6). Bars show means (± SEM). Statistical differences were assessed by two ways ANOVA (chronic and acute treatment). *** $P<0.001$ significant difference vs. chronic RANKL or insulin, $$$$ $p<0.0001$ significant difference vs. control (Ctl).

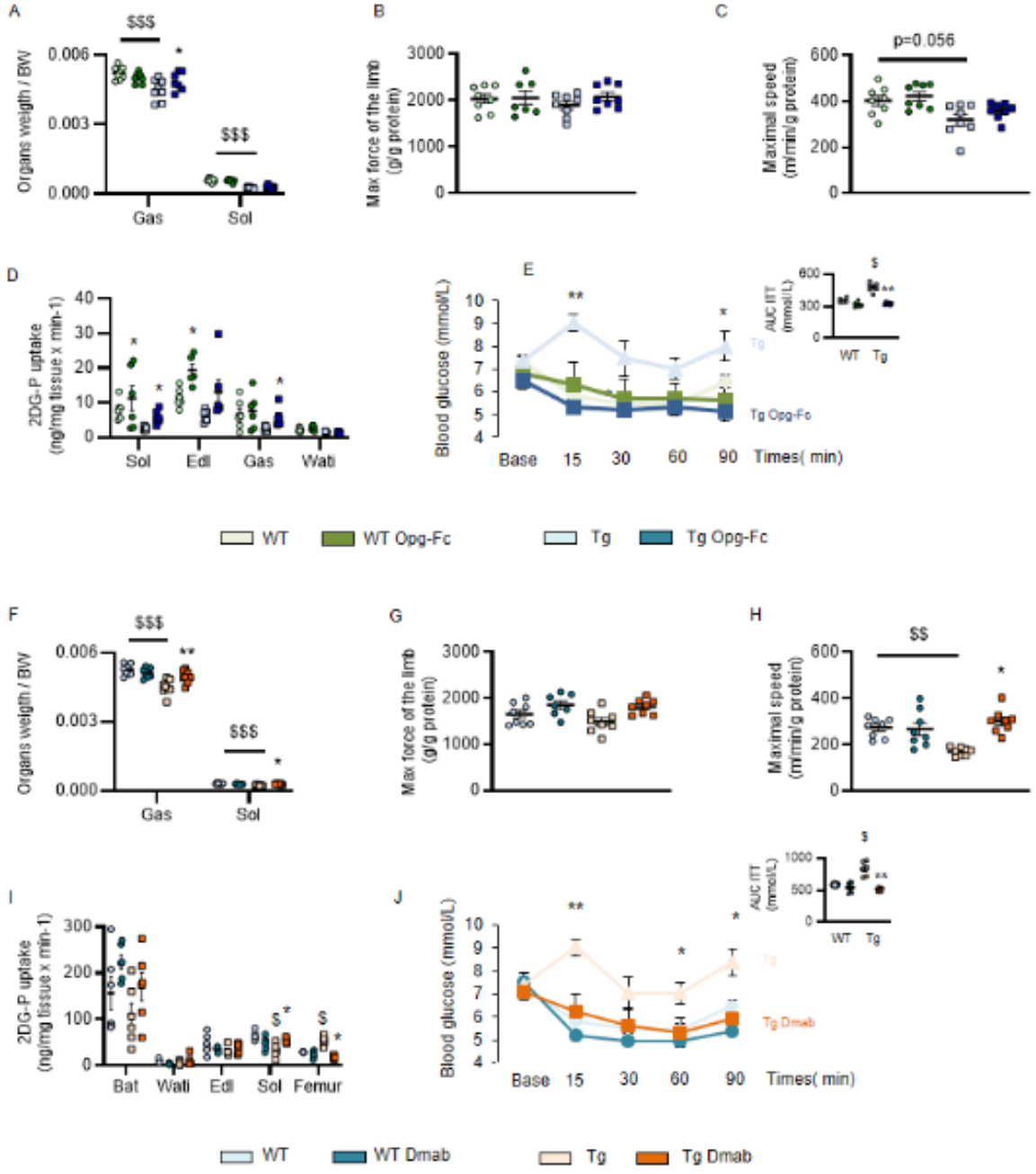

Fig. 5

Figure 5. Muscle and glucose phenotype of *huRANKLTg*+ (Tg) treated by OPG-Fc or Denosumab (Dmab). (A, F) Muscle mass normalized by body weight BW, *n* = 8 per group). (B, G) Limb force evaluated by handgrip normalized by gastrocnemius mass. (C, H) Maximal speed evaluated on treadmill normalized by gastrocnemius mass. (D, I) Tissue specific 2-[14C]deoxyglucose (2-[14C]DG) in soleus (Sol), E*xtensor digitorum longus* (Edl), Gastrocnemius (Gas), inguinal white adipose tissue (Wati) (*n* = 6 per group). (E, J) Insulin tolerance test (ITT), area under the curve (AUC) (*n* = 8 per group). The differences in control values from panels A to E to respectively F to J are due to studies separated in time by 1 year. Statistical differences were assessed by two ways ANOVA (genotype and treatment). * *P*<0.05, ** *P*<0.01, *** *P*<0.001 significant difference vs. saline. Bars show means (± SEM).

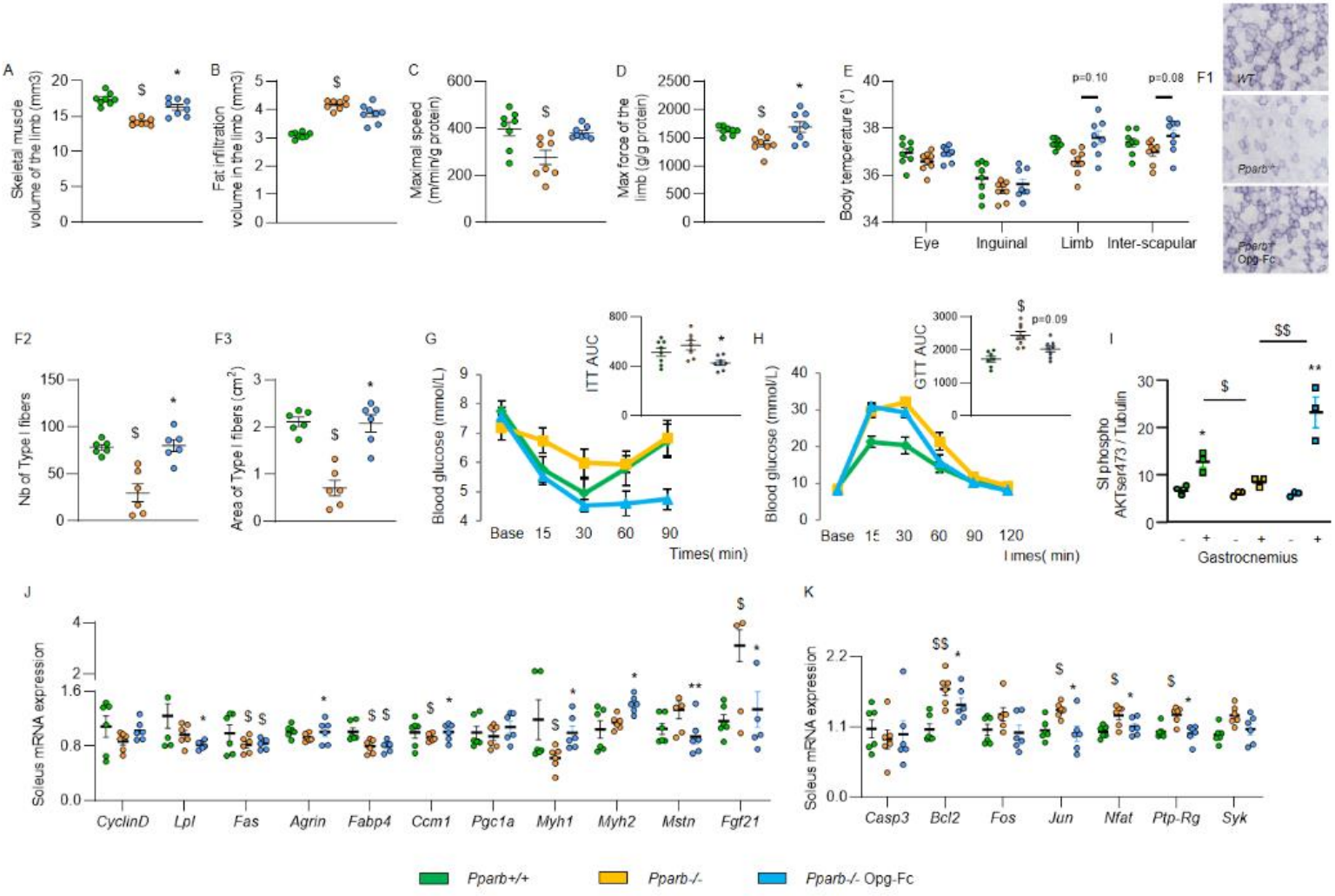

Fig. 6

Figure 6. Bone, muscle and glucose phenotype of *Pparb*$^{-/-}$ treated by OPG-Fc. (A-B) Skeletal muscle volume of the limb and fat infiltration in muscle evaluated by in vivo microCT. (C) Maximal speed evaluated on treadmill normalized by gastrocnemius mass. (D) Limb force evaluated by handgrip normalized by gastrocnemius mass (n = 8 per group). (E) Body temperature evaluated by infrared camera (n = 8 per group). (F) Muscle fiber type, number and area, note the type I fibers in blue dark and type II in light blue. (G) Insulin tolerance test (ITT), area under the curve (AUC) (n = 8 per group). (H) Glucose tolerance test (ITT). (I) Relative protein expression in the gastrocnemius, hatched bar correspond to mice which have received an acute injection of insulin. (J) Relative mRNA expression of insulin signaling in soleus. (K) Relative mRNA expression of *Nfkb* signaling in soleus. Statistical differences were assessed by one way ANOVA. * P<0.05, ** P<0.01, *** P<0.001 significant difference vs. saline. $ P<0.05, $$ P<0.01, $$$ P<0.001 significant difference vs. *WT*. Bars show means (± SEM).